

INFLUENCE OF CRYSTALLIZATION CONDITIONS ON THE NANO-/MICRO- BEHAVIOR OF CARBON FIBER-REINFORCED PEEK COMPOSITE

S. Vanpée^{1,2}, J. Chevalier³, B. Nysten² and T. Pardoën¹

¹ Institute of Mechanics, Materials and Civil engineering (iMMC), UCLouvain, Place Sainte-Barbe 2, 1348 Louvain-la-Neuve, Belgium

² Institute of Condensed Matter and Nanosciences (IMCN), UCLouvain, Croix du Sud 1, 1348 Louvain-la-Neuve, Belgium

³ Material Science Application Center, Solvay, Rue de Ransbeek 310, 1120 Brussels, Belgium

Keywords: PEEK composite, Crystallization, Micromechanics

ABSTRACT

In the context of the energy transition, the transportation sector faces the double challenge of producing lighter but higher-performance structural parts while improving their recyclability. Thermoset-based composite materials allow the manufacturing of light structures with excellent mechanical properties, but are very hardly recyclable and can only be processed via liquid molding techniques (e.g. vacuum infusion) or prepreg consolidation. Moreover, high-rate composite processing is impossible with such matrices: they require a curing step, which often lasts a few hours at high temperatures. Transitioning from thermoset to thermoplastic polymer matrix composites overcomes these shortcomings. However, this involves understanding how processing conditions influence the microstructure of the thermoplastic matrix and the mechanical performances of the composite.

Among thermoplastic polymers, semi-crystalline polymers like polyetheretherketone (PEEK) offer superior mechanical properties. The performances of PEEK-based composites are related to the amount and characteristics of the crystalline phase, which depend on the processing conditions. In this work, chemico-physical characterization techniques are combined with nano-/micro- mechanical tests to link the polymer microstructure to the mechanical response at the fiber/matrix level. The crystalline phase morphology is assessed through atomic force microscopy (AFM), scanning electron microscopy (SEM) as well as polarized optical microscopy (POM). The mechanical properties of the inter-/intra spherulitic and trans-crystallization zones are evaluated via nanoindentation (NI) tests. The knowledge of the crystal formation is used to guide the NI mapping, allowing identification of spherulite rich/poor regions around the fibers. The deformation and damage mechanisms occurring in the matrix at the micro-scale during transverse compression tests are studied using nano-digital image correlation (DIC).

1 INTRODUCTION

Thermoplastic composites have gained significant interest in, among others, aerospace, architecture, automotive, and marine applications associated to the potential of producing lightweight high-performance parts. Also, recyclability is possible compared to thermoset composites. However, the transition from thermoset to thermoplastic composites involves understanding how processing conditions influence the microstructure of the thermoplastic matrix, in particular, for the semi-crystalline thermoplastics, the trans-crystalline layer at the fiber/matrix interface, which in turn influences the mechanical performances of the composite.

The trans-crystalline layer has a highly oriented crystalline morphology at the fiber/matrix interface which developed during cooling of a semi-crystalline polymer matrix. This trans-crystalline layer develops under particular crystallization conditions only, in which the nucleating ability at the fiber surface/interface is higher than in the bulk matrix. For instance, it is reported that high crystallization temperature promotes trans-crystallization by increasing the nucleating ability of fibers [1]. Other

parameters influence the characteristics and extent of this trans-crystalline layer such as the pressure, cooling rate and the nature of the fiber/matrix system [2-5]. The latter mainly affects chain mobility and crystallization ability of polymer chains. The presence of a trans-crystalline layer at the fiber/matrix interface has shown to significantly impact the overall mechanical response of semi-crystalline thermoplastic composite including strength, modulus and fracture toughness [6-8]. Only few studies have been carried out to understand the impact of this trans-crystalline layer on the local mechanical behavior of the matrix confined in the inter-fiber zones. However, the understanding of the deformation and damage mechanisms at the fiber/matrix level helps linking the microstructure to the overall composite performances, which is required for composite performances optimization and for tailoring its properties with respect to specific applications.

This study focuses on the semi-crystalline polyetheretherketone (PEEK)/carbon fiber composites. The objective is to correlate PEEK matrix microstructure with the local mechanical response (deformation and damage mechanisms) of the composite at the fiber/matrix level. First, different microscopy characterization techniques (atomic force microscopy (AFM), scanning electron microscopy (SEM) and polarized light microscopy (POM)) were used for imaging the microstructure (i.e. spherulites and trans-crystalline layer) of the neat polymer (PEEK) and of the composite. Most of the techniques were first applied on the neat polymer for the sake of convenience (no perturbation due to fibers) and in order to generate a reference condition, followed by tests on ‘model samples’ (composite with few fibers) and on macroscopic composites. Second, the local mechanical properties and behavior of the polymer matrix were determined through nanoindentation and nano-digital image correlation (DIC). Nanoindentation is the most used characterization technique for determining local properties of polymers and their composites [9]. The nano-DIC method has recently been developed and enables to directly observe strain field at the micro scale during mechanical testing [10]. All the characterization techniques used on the different materials are summarized in Figure 1.

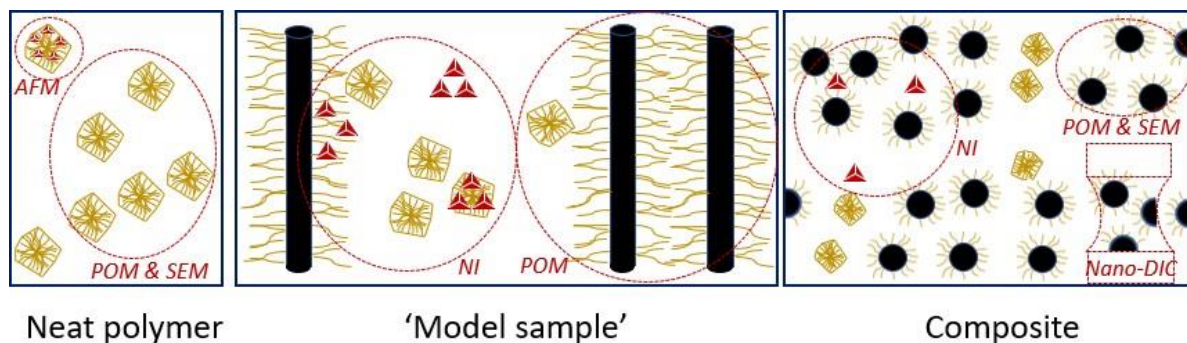


Figure 1: Scheme showing the microstructure and the different characterization techniques used for linking microstructure to mechanical response of the composite.

The sample preparation and characterization techniques are detailed in Section 2 followed by the results and discussions in Section 3. A short conclusion of this work is presented in Section 4.

2 MATERIALS AND METHODS

PEEK pellets, carbon fibers and the composite were all supplied by Solvay S.A.. The unidirectional (UD) carbon fiber reinforced PEEK composite slabs were manufactured by press-forming (*press Fontijne, LabPro 400*) in the standard conditions (i.e. as currently used at Solvay). The fiber weight

fraction is ~ 66%. Different types of samples were produced for the different characterization techniques.

For atomic force microscopy (AFM), PEEK pellets were first heated at 400°C for 5 minutes and then isothermally crystallized (310°C, 1h) in a differential scanning calorimeter (DSC) (*DSC 1, Mettler Toledo*) follow by ultramicrotome sectioning (*LIECA EM 8C6 microtome*) with a diamond blade at room temperature. In addition, some samples were then etched with a permanganate solution following the ICI procedure detailed in [11].

AFM was performed in Tapping mode (*Dimension Icon, Bruker Corp., USA*) using PPP-NCHR non-contact/tapping-mode probes (*Nanosensors, Switzerland*) with cantilever spring constant and resonance frequency values respectively around 42 N.m⁻¹ and 330 kHz and a nominal tip radius around 8 nm. AFM scans of 3 x 3 μm² and 10 x 10 μm² were generally performed with a setpoint amplitude around 15 nm (free amplitude around 20 nm) at a scan rate between 0.5 and 1.0 line/s.

Rectangular PEEK specimens were produced by injection moulding ($T_{Injection} = 380^{\circ}\text{C}$, $T_{Mould} = 80^{\circ}\text{C}$) (*FANUC, Roboshot, S-2000i150A*) for scanning electron microscopy (SEM) observations of the fracture surfaces of broken PEEK samples after liquid nitrogen immersion. Rectangular composite specimens were also cut from the previously consolidated plate, heated at 400°C for 5 minutes and then isothermally crystallized in the DSC (300°C, 15 min). In all cases, samples were first immersed in liquid nitrogen for 5 minutes and were then directly cold broken with pliers.

The fracture surfaces after liquid nitrogen fracturing were imaged on a *Zeiss Ultra 55 SEM*.

For polarized optical microscopy (POM), the three different samples (i.e. PEEK, ‘model samples’ and composite) were produced based on PEEK powders obtained after pellets grinding (*Pulverisette 14, Fritsch*). Grinding was needed to produce very thin film of PEEK for observations in transmitted light. The PEEK and composite films were processed by placing respectively the PEEK powder and a composite ply (~ 140 μm thick) in between 2 glass slides. ‘Model samples’ (composite with few fibers) were however manufactured by spreading PEEK powder on a glass slide on which some carbon fibers (same as in the composite) have been previously deposited. The powder and fibers were covered with an upper glass slide.

In all cases, the samples were heated at 400°C on a hot plate (*Ceran™, Gestigkeit Harry™ 4A*) and then isothermally crystallized on a heating plate (*FP90 Central Processor and FP82 hot stage, Mettler Toledo*) (300°C, 15 min).

POM observations were performed on an *Olympus AX70* light microscope in transmitted light mode. The *ImageJ software* was used for image processing.

For nanoindentation (NI), one type of sample was produced for each experiment. For the tests performed on ‘model samples’, these were similar to the ones used for POM observations except that a release agent was added on the upper glass slide to ease its withdrawal before testing. For tests in the matrix pockets, cubic composite specimens were cut from a consolidated plate. The samples were then polished in the direction perpendicular to the fibers using a *MultiPrep precision Polishing System (Allied High-Tech Products, Inc., Ca, USA)*.

The *Agilent G200* nanoindenter was used for nanoindentation experiments using a Berkovich tip with a half-angle opening of 65.3°. The indentation tests were performed at a rate of 0.05 s⁻¹ using the continuous stiffness measurement (CSM) mode to measure the hardness and modulus all along the test and the contact area was estimated using the Oliver and Pharr method [12].

For in-situ transverse compression tests followed by nano-DIC, dog-bone-shaped composite specimens were cut from a consolidated plate and then polished in the direction perpendicular to the fibers.

In-situ transverse compression tests were performed using a *Deben microtest* machine equipped with a 2 kN load cell inserted in an SEM, see [13]. A fine and dense speckle pattern of around 10 nm in size was deposited using electron beam evaporation of indium [10, 14, 15]. Images were taken all along the loading up to failure of the specimen following the procedure described in [10]. The DIC analyses were

performed with the open source *Ncorr* software. A subset size and a step size of respectively 12 pxl and 5 pxl were chosen.

3 RESULTS AND DISCUSSION

3.1 Microscopy characterization

Different characterization techniques were combined in order to map the microstructure (i.e. spherulites and trans-crystalline layers) of the matrix within the composite. Most of the techniques were first tried on the neat polymer (PEEK) and ‘model samples’ (composite with few fibers) for the sake of convenience (no perturbation due to fibers).

3.1.1 Atomic force microscopy

Atomic force microscopy was performed on etched and non-etched samples. The procedure developed by ICI for chemical etching showed that with the right etching parameters, topographic contrast can be obtained at the spherulite level due to the better chemical resistance of the crystalline lamellae compared to the amorphous phase in the inter and intra-spherulitic zones. The etching step potentially helps therefore to highlight the crystalline structure with the topographic contrast in AFM for example.

AFM images indicate that no permanganic etching is required for revealing the crystal microstructure of PEEK, as observed in Figure 2. In addition, when comparing AFM images of etched and non-etched samples, no significant difference can be observed regarding the spherulite morphology. This result leads to the conclusion that chemical etching is not an easily repeatable technique for spherulite characterization. Every little deviation of etching time, solution concentration and/or etching temperature from the procedure developed by ICI leads to the absence of real etching.

It is worth mentioning that AFM will later be performed on ‘model samples’ to check the validity of this technique for trans-crystalline layers observation.

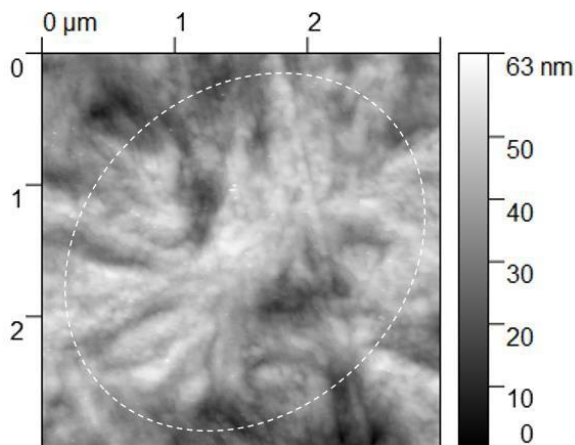


Figure 2: AFM image (topographic contrast) of a spherulite in a non-etched ultramicrotomed PEEK sample after isothermal crystallization (310°C, 1h). The approximate diameter of the spherulite is highlighted.

3.1.2 Scanning electron microscopy

SEM observations of the fracture surfaces of broken PEEK samples after liquid nitrogen immersion showed complex fracture surfaces (see Figure 3(a)), revealing the contour of spherulites (~1 μm diameter) but also regions with stretched matrix filaments, likely related to the presence of amorphous

polymer between spherulites. This method has already shown in the past to be efficient for morphology observation in other polymers [16].

The same methodology was then applied to the composite to reveal the trans-crystalline layer around the fibers. However, the observation of the crystalline phase in the composite by SEM was found quite difficult due to the high roughness of the fracture surfaces and to decohesion of the fiber/matrix interface both associated to the high fiber volume fraction (see Figure 3(b)).

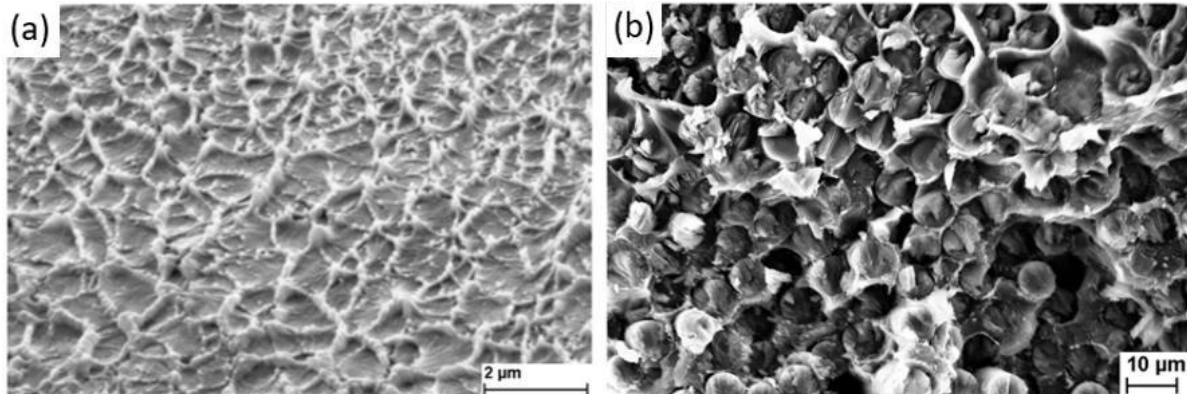


Figure 3: SEM micrograph of a fracture surface of PEEK (a) and the PEEK/C fibers composite (b) after fracture in liquid nitrogen

3.1.3 Polarized optical microscopy

POM in transmission mode was used to characterize the crystalline phase in isothermally crystallized PEEK samples, ‘model samples’ and composites. This technique easily maps the crystalline phase in pure PEEK samples and in the ‘model samples’ thanks to the birefringence phenomenon. However, as in the case of liquid nitrogen fracturing, the observations performed on the composites are much more complicated: the high fiber volume fraction coupled with the difficulties of manufacturing very thin PEEK films with fibers make the observations of spherulites and trans-crystallization phenomenon much more delicate.

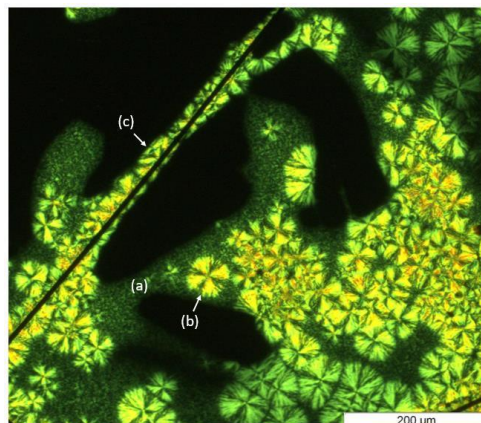


Figure 4: Polarized optical microscopy (POM) image of the ‘model’ carbon fiber-reinforced PEEK sample after isothermal crystallization (300°C, 15 min). The inter- and intra-spherulitic zones as well as the trans-crystalline layer are highlighted as (a), (b) and (c) respectively. No polymer is present in the black zones.

3.2 Nanoindentation

3.2.1 PEEK pockets in the composite

Nanoindentation in PEEK pockets of different sizes (i.e. at different distances from fibers) were performed to extract local PEEK properties in the vicinity of fibers. Figure 5 shows the variation of the modulus as a function of indentation depths for indents performed very close to fibers in small matrix pockets, in middle sized pockets and in large pockets. A clear increase of the modulus is observed near fibers, potentially due to the trans-crystallization phenomenon (the same observation is made based on the hardness-indentation depth curve). The distance between the indent and the fiber is, at such 100 - 200 nm distance from the fibers, large enough to avoid a mechanical constraint effect associated to the stiff fiber. The increase of modulus observed at high indentation depth for small resin pockets is due to the contact of the nanoindenter tip with the surrounding fibers.

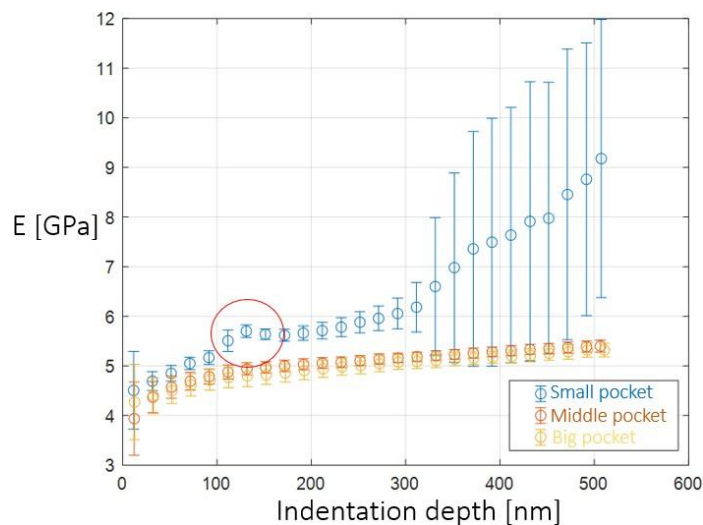


Figure 5: Modulus-indentation depth curves obtained by nanoindentation in resin pockets of different sizes (small, middle and big) in the composite. The peak of modulus at small indentation depth is highlighted with the red circle.

3.2.2 PEEK in ‘model samples’

Nanoindentation was also performed on ‘model samples’ in order to compare mechanical properties (i.e. hardness) of the different matrix phases (i.e. inter-/intra spherulitic and trans-crystallization zones) previously highlighted as (a), (b) and (c) in Figure 4. Figure 6 shows that the hardness of the trans-crystalline layer is ~65% higher than the one of spherulites at large indentation depth (i.e. 300 nm). This result still needs to be confirmed by performing rigorous finite element simulations: the impact of the fiber on the values obtained in the trans-crystalline layer cannot be ruled out due to the fiber proximity during testing. The same trend was observed on the modulus-indentation depth curve.

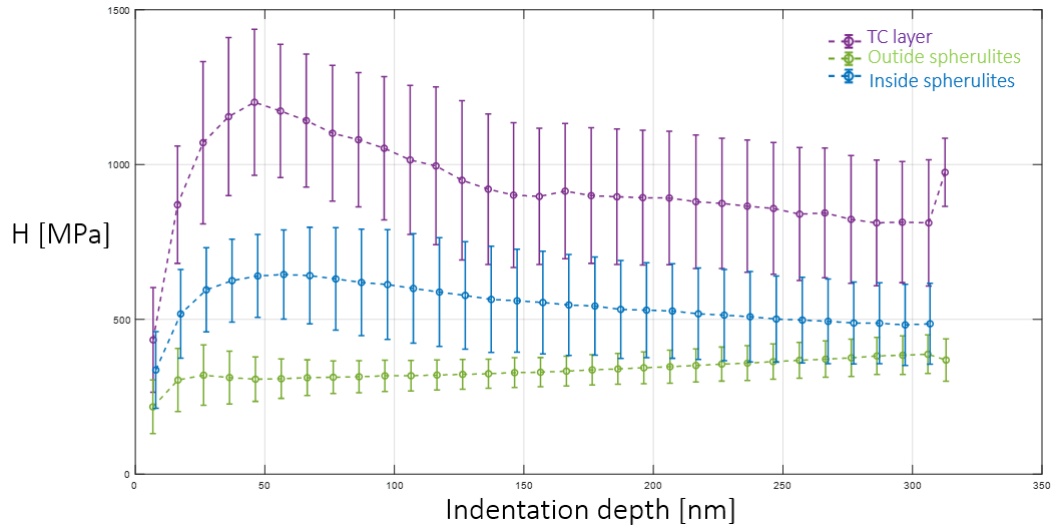


Figure 6: Hardness-indentation depth curves obtained by nanoindentation of the trans-crystalline layer (TC), inter- and intra-spherulitic zones (Outside and inside spherulites respectively) of a ‘model’ carbon fiber-reinforced PEEK sample isothermally crystallized (300°C, 15 min).

In addition, the intra-spherulitic zones (i.e. inside spherulites) show a higher hardness (~32% at 300 nm depth) compared to inter-spherulitic zones (i.e. outside spherulites). Both curves tend to the same hardness value at higher indentation depth due to properties homogenization of the inter and intra-spherulitic zones. The high standard deviations observed on the two upper curves can be explained by local variation of hardness within the same spherulite and within the trans-crystalline layer.

3.3 Nano digital image correlation

Transverse compression tests of the composite were performed in the SEM followed by nanoscale digital image correlation to track the evolution of the local strain field. The results show that the shear strain amplitude is the highest in a thin region (~300 nm) close to the fiber-matrix interface (see Figure 7), highlighting the heterogeneous strain field of PEEK during mechanical testing. In addition, this image shows that the local strain field can be determined at the fiber/matrix with this method.

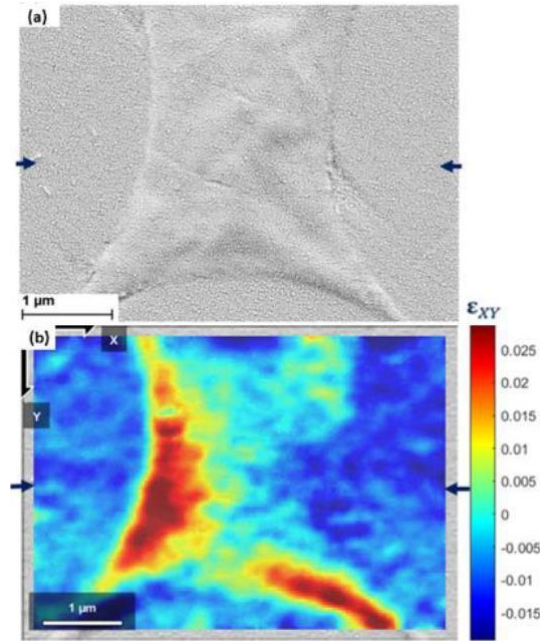


Figure 7: (a) SEM image after in-situ transverse compression of unidirectional carbon fiber-reinforced PEEK followed by nanoscale-digital image correlation (DIC). The speckle used for DIC is about 10-20 nm in size. (b) Corresponding shear deformation field (N_{corr}). The compression direction is indicated by blue arrows.

4 CONCLUSIONS

The crystallization of semi-crystalline polymers has been widely studied for the several decades [17-20]. However, the impact of the crystallization on the mechanical performances of composites is not yet fully understood, due to the presence of the trans-crystallization phenomenon. Many researches indicated a notable impact of trans-crystalline layers on the overall mechanical response on semi-crystalline based composites. Yet, too little researches have been done to determine the local fiber/matrix level mechanical response / the local mechanical behavior of the polymer matrix confined between fibers at the local scale which is crucial to correlate processing conditions with the performance of the final composite part. Hence, this work aims to combine microstructural characterization with nano-/micro-mechanical characterization in order to unravel the root cause of the change of performances from the smallest scale of relevance.

To this end, different microscopy characterization techniques were used to map the microstructure of the semi-crystalline polymer and determine the best method for polymer microstructure observation. The identification of the spherulite rich/poor regions around the fibers and the trans-crystallization regions on the fibers is used to guide nano-/micro-mechanical techniques mapping. With nanoindentation and nano-DIC method, local hardness, modulus and strain fields can be extracted for the different polymer matrix phases (i.e. inter-/intra spherulitic and trans-crystallization zones) within the composite. The main results of this ongoing study are the following:

- The different microscopy characterization techniques investigated for polymer microstructure mapping proved successful when applied on the neat resin, in particular the polarized optical microscopy technique. Yet, in the case of the composite, observations are much more delicate due to high fiber volume fraction in the composite.
- Nanoindentation in resin pockets indirectly highlights the presence of a potential trans-crystalline layer in the composite. An increase of elastic modulus is found near the fibers. This is important in the context of understanding and predicting the load transfer through the fiber-matrix interface.

- Nanoindentation in ‘model samples’ showed variations of mechanical properties (hardness and modulus) of the different resin phases (i.e. inter-/intra spherulitic and trans-crystallization zones). The trans-crystalline layer exhibits higher hardness values compared to the intra-spherulitic zones, which reveals itself a higher hardness compared to inter-spherulitic zones.
- Nano-DIC is able to capture the very local strain field developing in the near fiber/matrix region, which very much dictates the possible decohesion process.

In general, this work shows the first results aiming to correlate polymer microstructure with its nano-/micro- mechanical response. The combination of polymer microstructure mapping with local mechanical characterization and direct strain measurements is still missing.

Future work includes varying processing conditions for generating other polymer microstructures and characterize with the most appropriate microscopy techniques. The impact of processing conditions on the nano-/micro- mechanical behavior of the polymer matrix will also be investigated.

ACKNOWLEDGEMENTS

SV is a researcher of the Financements Région de Bruxelles-Capitale (Innoviris) and gratefully acknowledges their support. All the ressources have been provided by the Institute of Mechanics, Materials and Civil engineering (iMMC), Institute of Condensed Matter and Nanosciences (IMCN) of the Université catholique de Louvain (UCLouvain) and Solvay S.A. (Brussels) funded by the Financements Région de Bruxelles-Capitale (Innoviris).

REFERENCES

- [1] W. Wang, Z. Qi and G. Jeronimidis, Studies on interface structure and crystal texture of poly(ether-ether-ketone)-carbon fibre composite, *Journal of Materials Science*, **26**, 1991, pp. 5915-5920 (<https://doi.org/10.1007/BF01130134>).
- [2] J.P. Abdou, G.A. Braggin, Y. Luo, A. R. Stevenson, D. Chun and S. Zhang, Graphene-Induced Oriented Interfacial Microstructures in Single Fiber Polymer Composites, *ACS Applied Materials & Interfaces*, **7**, 2015, pp. 13620-13626 (<https://doi.org/10.1021/acsami.5b03269>).
- [3] E.J.H. Chen and B.S. Hsiao, The Effects of Transcrystalline Interphase in Advanced Polymer Composites, *Polymer Engineering and Science*, **4**, 1992, pp. 280-286 (<https://doi.org/10.1002/pen.760320408>).
- [4] C. Wang and C.-R. Liu, Transcrystallization of polypropylene composites: nucleating ability of fibres, *Polymer*, **40**, 1999, pp. 289-298 ([https://doi.org/10.1016/S0032-3861\(98\)00240-7](https://doi.org/10.1016/S0032-3861(98)00240-7)).
- [5] H. Quan, Z.-M Li, M.-B. Yang and R. Huang, On transcrystallinity in semi-crystalline polymer composites, *Composites Science and Technology*, **65**, 2005, pp. 999-1021 (<https://doi.org/10.1016/j.compscitech.2004.11.015>).
- [6] S.-L. Gao and J.-K. Kim, Cooling rate influences in carbon fibre/PEEK composites. Part II: Interlaminar fracture toughness, *Composites Part A*, **32**, 2001, pp. 763-774 ([https://doi.org/10.1016/S1359-835X\(00\)00188-3](https://doi.org/10.1016/S1359-835X(00)00188-3)).
- [7] Y. Lee and R.S. Porter, Crystallization of poly(etheretherketone) (PEEK) in carbon fiber composites, *Polymer Engineering and Science*, **26**, 1986, pp. 633-639 (<https://doi.org/10.1002/pen.760260909>).
- [8] S.-L. Gao and J.-K. Kim, Cooling rate influences in carbon fibre/PEEK composites. Part III: impact damage performance, *Composites Part A*, **32**, 2001, pp. 775-785 ([https://doi.org/10.1016/S1359-835X\(00\)00189-5](https://doi.org/10.1016/S1359-835X(00)00189-5)).
- [9] T. Pardoën, N. Klavzer, S. Gayot, F. Van Loock, J. Chevalier, X. Morelle, V. Destoop, F. Lani, P.P. Camanho, L. Brassart, B. Nysten and C. Bailly, Nanomechanics serving polymer-based composite research, *Comptes Rendus. Physique*, **22**, 2021, pp. 331-352 ([10.5802/crphys.56](https://doi.org/10.5802/crphys.56)).
- [10] N. Klavzer, S.F. Gayot, M. Coulombier, B. Nysten and T. Pardoën, Nanoscale digital image

- correlation at elementary fibre/matrix level in polymer-based composites, *Composites Part A*, **168**, 2023 (<https://doi.org/10.1016/j.compositesa.2023.107455>).
- [11] A. Jonas, *Structural features of semi-crystalline poly(ether ether ketone): extension to composite materials*, Université Catholique de Louvain, Louvain-la-Neuve, 1992.
- [12] W.C. Oliver and G.M. Pharr, An improved technique for determining hardness and elastic modulus using load and displacement sensing indentation experiments, *Journal of Materials Research*, **7**, 1992, pp.1564-1583 (<https://doi.org/10.1557/JMR.1992.1564>).
- [13] J. Chevalier, P.P. Camanho, F. Lani and T. Pardoën, Multi-scale characterization and modelling of the transverse compression response of unidirectional carbon fiber reinforced epoxy, *Composite structures*, **209**, 2019, pp.160-176 (<https://doi.org/10.1016/j.compstruct.2018.10.076>).
- [14] J. Hoefnagels, M. van Maris and T. Vermeij, One-step deposition of nano-to-micron-scalable, high-quality digital image correlation patterns for high-strain in-situ multi-microscopy testing, *Strain*, **55**, 2019 (<https://doi.org/10.1111/str.12330>).
- [15] L.P. Canal, C. González, J.M. Molina-Aldareguía, J. Segurado and J. Llorca, Application of digital image correlation at the microscale in fiber-reinforced composites, *Composites Part A*, **43**, 2012, pp. 1630-1638 (<https://doi.org/10.1016/j.compositesa.2011.07.014>).
- [16] A.K. Kulshreshtha, G.C. Pandey, S.F. Xavier and J.S. Anand, SEM fractographic studies on PVC/ABS polyblends, *European Polymer Journal*, **25**, 1989, pp. 925–927 ([https://doi.org/10.1016/0014-3057\(89\)90111-0](https://doi.org/10.1016/0014-3057(89)90111-0)).
- [17] Y. Wang, J.D. Beard, K.E. Evans and O. Ghita, Unusual crystalline morphology of Poly Aryl Ether Ketones (PAEKs), *RSC Advances*, **6**, 2016, pp. 3198-3209 ([10.1039/C5RA17110E](https://doi.org/10.1039/C5RA17110E)).
- [18] L. Jin, J. Ball, T. Bremner and H.-J. Sue, Crystallization behavior and morphological characterization of poly(ether ether ketone), *Polymer*, **55**, 2014, pp. 5255-5265 (<https://doi.org/10.1016/j.polymer.2014.08.045>).
- [19] X. Tardif, B. Pignon, N. Boyard, J.W.P. Schmelzer, V. Sobotka, D. Delaunay and C. Schick, Experimental study of crystallization of PolyEtherEtherKetone (PEEK) over a large temperature range using a nano-calorimeter, *Polymer Testing*, **36**, 2014, pp. 10-19 (<https://doi.org/10.1016/j.polymertesting.2014.03.013>).
- [20] Y. Furushima, C. Schick and A. Toda, Crystallization, recrystallization, and melting of polymer crystals on heating and cooling examined with fast scanning calorimetry, *Polymer crystallization*, **1**, 2018 (<https://doi.org/10.1002/pcr2.10005>).